Available online at www.sciencedirect.com

ScienceDirect

Energy Procedia 1 (2009) 3885–3892

Energy Procedia

www.elsevier.com/locate/procedia

GHGT-9

High temperature behavior of NiO-based oxygen carriers for Chemical Looping Combustion

Rein Kuusik[a], Andres Trikkel[a,*], Anders Lyngfelt[b], Tobias Mattisson[b]

[a]*Tallinn University of Technology, Ehitajate 5, 19086 Tallinn, Estonia*
[b]*Chalmers University of Technology, S-412 96 Göteborg, Sweden*

Abstract

High temperature behavior of spray-dried NiO-based oxygen carrier samples for Chemical Looping Combustion (CLC) under oxidizing and reducing conditions was studied using a ceramic fluidized bed furnace. Differently from the common CLC process, high enough temperatures were obtained by burning air and methane mixture directly in the bed of carriers, changing the stoichiometric air to fuel ratio in the range of 0.70 to 1.30 and using external electric heating.

None of the five particle samples tested showed any sign of defluidization in oxidizing atmosphere at any of the temperatures tested, i.e. up to 1175-1185°C. However, under reducing conditions or in the oxidizing-reducing sequences, shortly after changing the atmosphere from oxidative to reducing, some of the spray-dried samples agglomerated causing defluidization. To study the structure of the carrier particles and to clarify the agglomeration phenomena, SEM and EDX analysis of the initial and treated samples was carried out. It was shown that agglomerates are formed through small bridges between the particles which consist of pure Ni phase. Three samples which were produced using MgO as an additive were tested. For these no defluidization was observed at any of the temperatures tested, i.e. up to 1175-1185°C, neither in oxidizing, nor in reducing atmosphere. So, addition of proper components to the carrier particles can significantly improve reliability of the CLC process at higher temperatures.

Keywords: chemical looping combustion; oxygen carrier; nickel; temperature resistance; agglomeration; defluidization

1. Introduction

Energy production based on combustion of fossil fuels results in increasing emissions of CO_2 which is considered the most important greenhouse gas. Reduction of anthropogenic CO_2 emissions is necessary to avoid global warming. This could be achieved by reducing the use of fossil energy sources and increasing the role of renewable energy, such as wind power or biofuels, or by improving the efficiency of energy conversion and its use. One option is also implementation of carbon capture and storage technologies. However, capture technologies are associated with significant energy penalties and costs, whereas the costs associated with geological storage are normally

* Corresponding author. Tel.: +372 620 2812
E-mail address: atrik@staff.ttu.ee

doi:10.1016/j.egypro.2009.02.191

expected to be smaller. An alternative to geological storage could be mineral carbonation with different silicates if the reactions can be improved [1, 2].

A novel combustion technology using CLC has been proposed to separate CO_2 efficiently from other flue gas components (N_2, unused O_2) already during combustion. CLC uses metal oxide particles for oxygen transport from combustion air to fuel, featuring 100% CO_2 capture – a highly concentrated CO_2 stream which is ready for sequestration [3, 4].

In CLC the gaseous fuel is introduced to one fluidized bed reactor (*fuel reactor*) where oxygen carrier particles are reduced according to:

$$(2n + m)MeO + C_nH_{2m} \rightarrow (2n + m)Me + mH_2O + nCO_2 \quad (1)$$

and gaseous fuel is converted to a stream of CO_2 and H_2O. Pure CO_2 can be obtained when H_2O is condensed. The reduced metal oxide is circulated to another fluidized bed reactor (*air reactor*) where metal is oxidized in an exothermic reaction according to:

$$Me + 1/2O_2 \rightarrow MeO \quad (2)$$

The flue gas from this reactor contains N_2 and unreacted O_2. The main advantage as compared to conventional combustion processes is that CO_2 obtained is not diluted with N_2. Most experimental work has been focused on oxygen carriers containing nickel, iron, manganese or copper oxide [3, 5, 6].

Fluidized beds operate at high temperatures and one possible problem could be defluidization due to agglomerate formation in the bed of particles, especially, at higher temperatures and lower gas velocities [7]. To scale up the CLC process and technology for industrial application and improve safety of the process, information about the high temperature resistance of oxygen carriers produced using commercially available methods and raw materials is needed. By temperature resistance is meant the ability to withstand high temperatures without defluidizing or agglomerating. In the present paper high temperature behavior of some spray-dried NiO-based oxygen carrier samples was studied at elevated temperatures under oxidizing and reducing conditions and possible agglomeration mechanism was clarified.

2. Experimental

Comprehensive testing with a number of oxygen carrier samples was performed in the frames of the EU project "CLC Gas Power – Chemical Looping Combustion" in order to define suitable conditions for spray-drying and to select particles with optimum parameters for CLC. Some of these materials were selected for further testing at significantly increased temperature. Characterization of the selected samples is given in Table 1.

The samples were prepared from the commercially available raw materials (mainly refractory grade NiO from Novamet and Al_2O_3 CT3000SG from Almatis) which showed the best results in laboratory testing. The particles were prepared by spray-drying at VITO NV, Flemish Institute for Technological Research, using the following procedure. Water-based slurry was prepared from the raw materials with small amounts of organic binders and dispersants. The slurry was mixed and milled and pumped into the spray dryer (NIRO 6.3-N SD, Denmark). After drying the particles were sintered at different temperatures and sieved to separate 106-212 μm fraction. XRD analysis showed that during sintering Al_2O_3 reacted with NiO to form $NiAl_2O_4$ and the composition of the particles was about 40% of NiO and 60% of $NiAl_2O_4$.

High temperature testing was carried out using a ceramic fluidized bed furnace with inner diameter 40 mm (Figure 1).

Table 1. Characterization of the samples and noticed defluidization

Notation	Characterization	Properties	Defluidization
S2	Novamet refractory grade NiO and Almatis CT3000SG Al_2O_3. Sintered 4h at 1450°C, 40% NiO, 60% $NiAl_2O_4$	BET surface area 0.34 m^2/g, porosity 0.40 mm^3/g**	**yes** (above 1050°C)
S3*	Similar to S2 (40% NiO)	BET surface area 0.66 m^2/g, porosity 0.83 mm^3/g	**yes** (above 1125-1150°C)
S8	Similar to S2 and S3 (40% NiO), but with 5% MgO (MagChem 30) added during preparation	BET surface area 0.91 m^2/g, porosity 1.04 mm^3/g	**no** up to 1185°C
S14	Novamet refractory grade NiO, Almatis AR78 $MgAl_2O_4$. Prepared to obtain 40% NiO. Sintered 4 h at 1400°C	BET surface area 0.41 m^2/g, porosity 0.49 mm^3/g	**no** up to 1185°C
S15	Similar to S2 and S3 (40% NiO), but with 10% MgO (MagChem 30) added during preparation. Sintered 4 h at 1400°C	BET surface area 0.92 m^2/g, porosity 1.08 mm^3/g	**no** up to 1185°C

* Sample S3 was selected for pilot scale experiments in 100 kW unit
**Porosities determined for the pore diameter range 1.5-30 nm by N_2 adsorption method

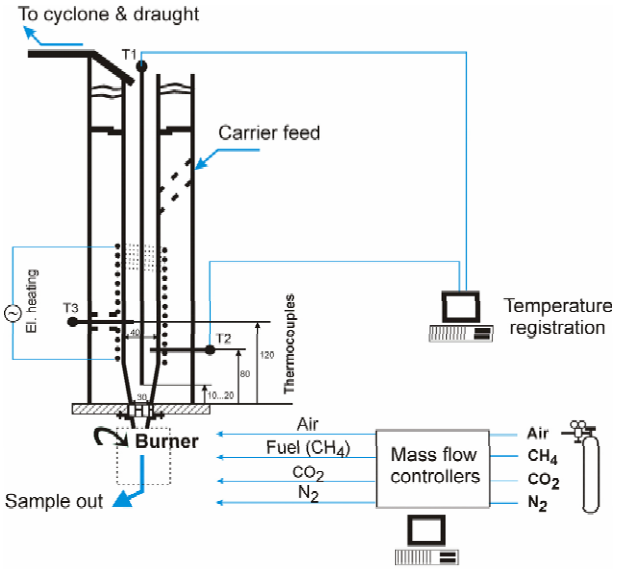

Figure 1. Scheme of the fluidized bed device for high temperature tests

The FB furnace was equipped with temperature control system and software for determining the temperature fields in the furnace. Digital mass-flow controllers and computerized control over the process to adjust the atmosphere in the furnace was used to quickly switch between oxidizing and reducing conditions in the bed of particles. The furnace was also equipped with air and inert gas pre-heater and cyclone for separation of solid particles from flue gas. To improve the heat balance, the furnace was equipped with an external electric heating system. This allowed carrying out tests at fluidization velocities w in the furnace 0.5-0.6 m/s both under oxidizing and reducing conditions. It was determined that at fluidization velocities over 0.6 m/s carry-out of particles from the reactor significantly increased. However, fluidization velocities near to maximum were necessary to achieve sufficiently high temperatures in the sample-bed. So, most of the experiments were carried out at fluidization velocities w=0.50-0.55 m/s.

The tests did not follow exactly the common cyclic batch testing of particles where gaseous fuel (CH_4) is alternated with air, or O_2 in N_2. Instead, “air reactor” and “fuel reactor” conditions were simulated by switching

between burning methane at over- and under stoichiometric conditions, the stoichiometric air ratio, α, typically changing between 1.3 and 0.7. To determine the behavior of particles at higher temperatures this variation could be considered reasonable, as the periods at high air ratio will provide conditions for oxidizing the particles, whereas the periods at low air ratio provides conditions for the reduction of the particles, the reducing gases being here H_2 and CO (and some unreacted CH_4). Composition of the gases at different values of α was calculated assuming equilibrium of reaction (3) with respective equilibrium constant (Eq. 4), and in combination with mass balance of the combustion reaction (Eq. 5):

$$CO_2(g) + H_2(g) \leftrightarrows CO(g) + H_2O(g) \quad (3)$$

$$K^T = \frac{[CO]\ [H_2O]}{[CO_2]\ [H_2]} \qquad (K^{1173K} = 1.306) \quad (4)$$

$$CH_4 + 2(O_2 + 3.76N_2) \rightarrow CO_2 + 2H_2O + 2 \cdot 3.76\ N_2 \quad (5)$$

Calculation results are given in Table 2. It can be seen that the content of reducing gases at α = 0.70 is about 14.5%. On the basis of thermogravimetric analysis of the products obtained in the tests under reducing conditions, it was found that almost 100% conversion of NiO to Ni can be achieved during 10-15 minutes at α = 0.70 and, partly, also $NiAl_2O_4$ was reduced. Particles were oxidized at an air to fuel ratio α ≈ 1.30 (about 5% of O_2 in gases) and it took up to 5 minutes to oxidize fully reduced particles.

Table 2. H_2 and CO content (% Vol) in flue gases at different values of α

Temperature	Gas	α = 0.85	α = 0.80	α = 0.70
1000°C	H_2	3.63	5.12	8.64
	CO	2.76	3.75	5.88
	Sum:	6.39	8.87	14.52
1100°C	H_2	3.36	4.78	8.21
	CO	3.03	4.09	6.31
	Sum:	6.39	8.87	14.52

In the tests the main parameter registered was temperature of the sample bed. The main thermocouple (T1, Figure 1) was placed in the hottest region of the furnace inside the sample-bed, i.e. 15±5 mm from the gas distributor. About 25-30 mL of the sample was used in the tests which corresponds to a bed height of ~25 mm of still bed. The sample was fed slowly under oxidizing conditions at α ≈ 1.30. The pressure drop (gas distributor + sample bed) was 40-55 mm H_2O during fluidization and it dropped sharply when defluidization took place. Behavior of the sample and pressure drop fluctuations were continuously monitored. Temperatures at 80 and 120 mm height from the gas distributor (T2 and T3) were also registered and served mostly for adjusting electric heating and obtaining information about the temperature field along the height of the furnace.

To control temperature in the course of the tests, air to fuel ratio α, fluidization velocity of gases w and voltage of electric heating and air pre-heater were manipulated if necessary. The experiments involved switching between periods of oxidizing and reducing conditions at different base (minimum) temperatures. The duration of these periods varied, but was typically 10-15 minutes. An example of a temperature profile of a test with sample S3 is presented on Figure 2. Note the significant reduction in temperature as particles are fed. The first reducing period is started after base temperature has been reached.

After reduction period when switching to α > 1, there is normally a sharp temperature increase in the bed. This phenomenon was used in the experiments to reach higher temperatures. So, switching back to reducing conditions was performed at definite temperatures of this peak – 1125, 1150, 1175°C or at the maximum temperature of the peak (1142°C on Figure 2). Thus, it was possible to follow stability of fluidization during the highest temperatures of the particle bed in the beginning of reduction, the slow decrease of temperature to the base temperature after switching to reducing conditions lasted about 3-5 minutes.

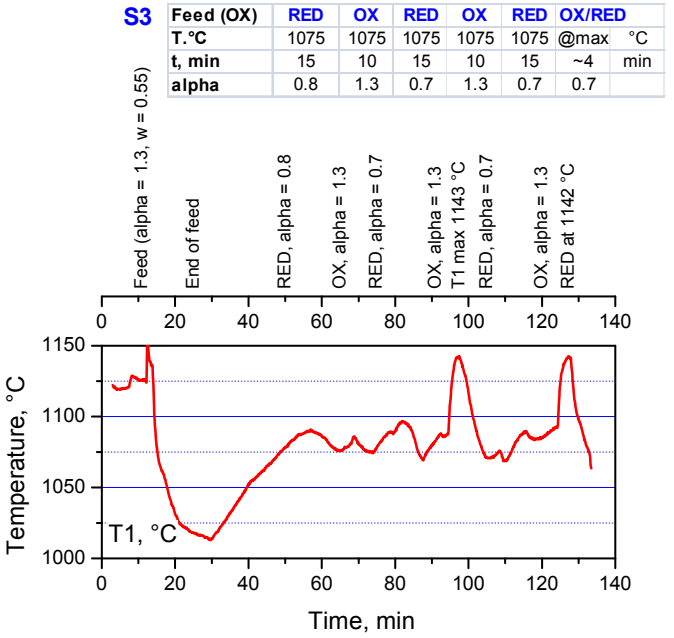

Figure 2. Temperature profile of a test, sample S3. Base temperature 1075°C, oxidizing and reducing sequences, switching from oxidizing (OX) to reducing conditions (RED) at base temperature and also at maximum peak temperature 1142°C

3. Results and discussion

Using SEM and EDX analysis methods the structure of the oxygen carrier particles S2, S3 and S8 was studied (Figure 3). It was noticed that many of the S2 and S3 particles were hollow inside, which can affect their strength and reduce density. Particles of S8 were more uniform.

When comparing surface of the samples (Figure 3) it can be seen that sample S2 differs from S3, the former having smooth surface, bigger crystals, signs of molten phase and less porosity. It can be noticed even more from the cross section photos on Figure 3. Crystals inside the S2 particle form uniform agglomerates and melts, whereas for the other samples they are more easily distinguishable and create more porosity. Sample S8 did not differ much from S3, however, porosity was even more expressed. BET specific surface area of the samples was 0.34, 0.66 and 0.91 m^2/g for S2, S3 and S8, respectively. At higher sintering temperatures (1450°C) liquid or molten phases may form inside the particles which can reduce porosity, increase diffusion resistance and diminish their reaction ability. It has also been noticed that particles sintered at higher temperatures agglomerate or defluidize more easily [7].

Element mapping of the particles showed that NiO was evenly distributed all over the cross section, not concentrated on the surface or in bigger spots. $NiAl_2O_4$ was also distributed evenly, but was associated with larger crystal sizes (darker areas on SEM photos). MgO in S8 was finely distributed over the particle. Element analysis indicated that the main elements present in S2 and S3 were Ni and Al, besides, small amount (~0.5%) of Co and Fe in traces.

There were no problems with agglomeration or defluidization of the bed or any deviations in the behavior of the sample bed under oxidizing ("*air reactor*") conditions, in any of the tests, not even at the maximum temperatures achieved in the device used (1175-1185°C). In addition, when small pressure drops were noticed during reduction sequence (in two tests with S3), the agglomerates possibly formed were broken after switching to oxidizing conditions as the pressure drop increased again and no agglomerates were noticed in the particle bed after experiment.

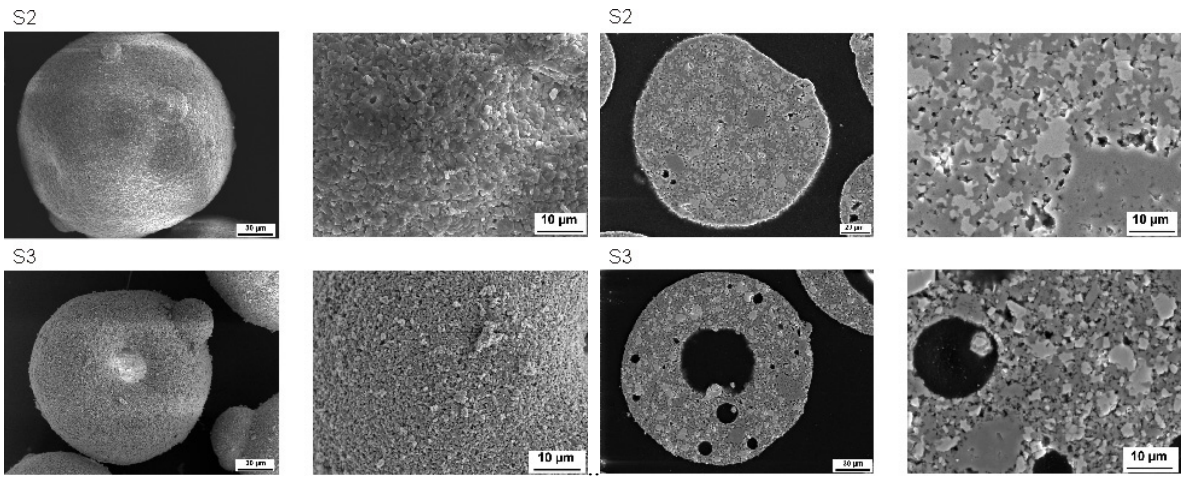

Figure 3. SEM photos of the carrier particles S2 and S3. Surface of the particles (left) and cross section (right)

It was found that the reduction process with sample S2 proceeded without defluidization at 1000°C and at 1050°C (α was 0.85 or 0.80 during reduction). In the test with S2, if the temperature was increased during the second oxidation period up to 1150°C and then switched to reducing atmosphere (α = 0.70), a sharp and complete defluidization of the bed material took place shortly after the switch. At the same time ΔP fell to 15 mm H_2O and ΔP fluctuations disappeared. The second test series with S2 was made at the lower temperature, 1050°C. During the first reducing period at this temperature no indication of defluidization was seen, whereas during the second switch to reducing conditions at 1050°C, the bed also instantly defluidized.

This shows that sample S2 has a clear tendency to defluidize under reducing conditions at temperatures already around 1050°C. Photos were taken of the agglomerates formed in the bed after opening the furnace (Figure 4). There were some small agglomerates in the bed at lower temperature (1050°C) and quite hard big agglomerate on the gas distributor formed at 1150°C. The agglomerates found after the experiment at lower temperature were not sufficiently hard to explain the defluidization, and most likely they broke down during or before opening of the reactor.

Both samples were analyzed also by SEM to further investigate the agglomerate formation mechanism. It can be seen (Figure 4) that at 1150°C plenty of molten phase is present on the surface. Several cuts along the cross-section were made to find exactly the level of some connection between the agglomerated particles. As can be seen in Figure 4, the bridges formed between the particles are quite small, which may explain the weakness of the agglomerates – they can be very easily broken. So, it may be assumed that the bridges between agglomerated particles were formed through molten Ni phase. However, melting temperature of pure Ni is high (1455°C) and taking into account that defluidization took place shortly after switching to reducing media when most of Ni should be present as NiO, these assumptions need additional control, including also analysis of eutectics in the system Ni – NiO – $NiAl_2O_4$.

To determine the composition of the bridges found, analysis was carried out using high resolution scanning electron microscope (Zeiss ULTRA 55) equipped with the In-Lens SE detector for topographic imaging and energy and angle selective backscattered detector for compositional contrast. The chemical composition of the films was determined using an energy dispersive X-Ray analysis (Röntec EDX XFlash 3001 detector).

As can be seen from Figure 5, composition of the connecting bridge corresponds to pure Ni phase, as determined in the middle of the bridge. The crystals around Ni phase near the surface of the particle (Figure 5) were $NiAl_2O_4$, as determined from the Ni : Al ratio ~1 : 2. This supports the finding that agglomerates are formed through molten Ni phase which is mainly formed from NiO during reduction stage or present in the particle due to incomplete oxidation during oxidation stage.

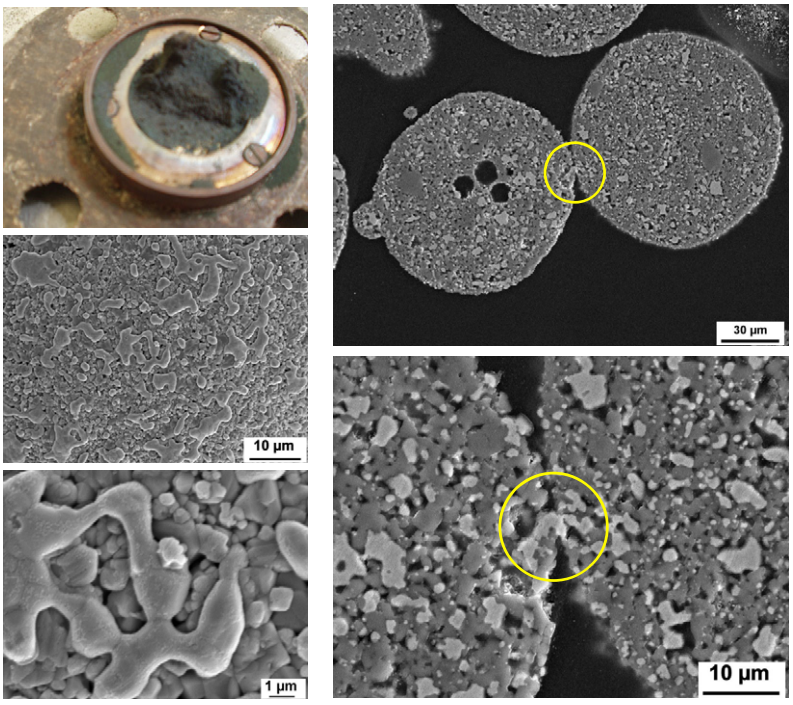

Figure 4. S2 particles which defluidized at 1150°C. Top left: agglomerate on the gas distributor; Left: surface of a particle; Right: cross section of two particles connected with a "bridge"

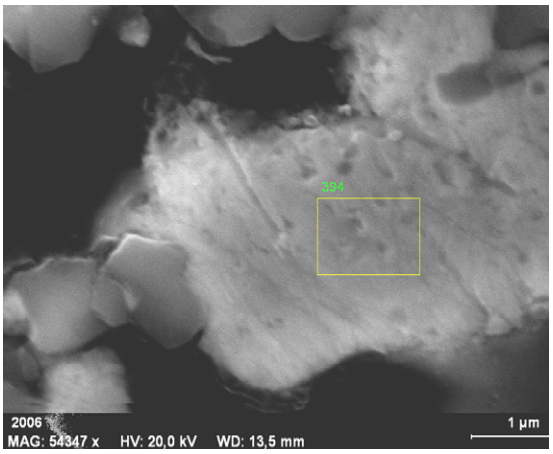

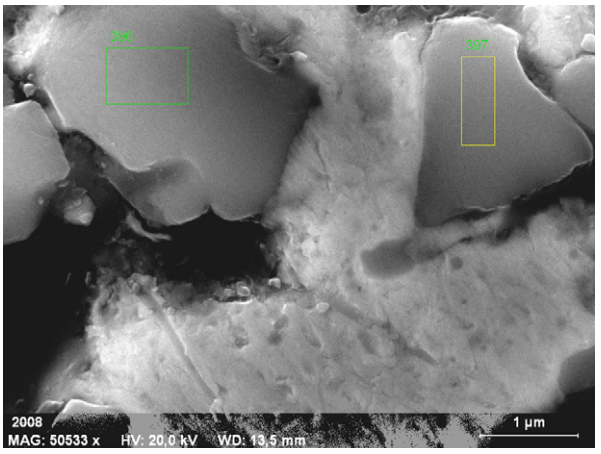

Spectrum: 394

Element	Series	unn. C [wt.-%]	norm. C [wt.-%]	Atom. C [at.-%]
Nickel	K-series	77,81	100,00	100,00
Total:		77,81	100,00	100,00

Spectrum: 396 (much O_2)

Element	Series	unn. C [wt.-%]	norm. C [wt.-%]	Atom. C [at.-%]
Nickel	K-series	34,68	50,90	32,28
Aluminium	K-series	33,45	49,10	67,72
Total:		68,12	100,00	100,00

Figure 5. SEM-EDX analysis of the composition of the bridges between agglomerated particles

Sample S3 also defluidized in some tests, but at higher temperatures – above 1125-1150°C. The main difference between the particles is their BET surface area and porosity, being lower for S2 (Table 1). So, considering structure of these particles (Figure 3), porosity data and results of testing, sintering temperatures above 1400°C should not be recommended for spray-dried CLC particles without MgO addition.

In order to improve particle properties, some carrier samples were made using MgO as an additive (samples S8, S14, S15). These particles did not form agglomerates or defluidize in any of the tests up to 1175-1185°C, neither in oxidizing nor in reducing conditions. So, addition of MgO clearly increased temperature resistance of the particles.

A summary of the test results is given in the right-hand column of Table 1.

4. Conclusions

High temperature behavior of several spray-dried NiO-based oxygen carrier samples for CLC combustion under oxidizing and reducing conditions was studied using a ceramic fluidized bed furnace. It was shown that in oxidizing atmosphere all the samples tested were thermally stable at all temperatures tested, i.e. up to 1175-1185°C. Under reducing conditions or in the oxidizing-reducing cycles, shortly after changing the atmosphere from oxidative to reducing, one of the five samples formed agglomerates or defluidized already at temperatures of around 1050°C. Another sample formed agglomerates or defluidized at temperatures around 1125-1150°C.

The three samples prepared with MgO as additive, did not form agglomerates or defluidize in any of the tests at any temperature tested, i.e. up to 1175-1185°C, neither in oxidizing nor in reducing conditions.

SEM and EDX analysis of the initial and treated samples was carried out to study the structure of the carrier particles used and to clarify the agglomeration phenomena. It was shown that agglomerates were formed through small connecting bridges between the particles which consisted of pure Ni phase.

Acknowledgements

This work was supported by EU project "Chemical Looping Combustion CO_2 Ready Gas Power", contract 019800, lead by Chalmers University of Technology. The authors also wish to thank Dr. Valdek Mikli and Dr. Olga Volobujeva from Tallinn University of Technology for carrying out SEM and EDX analysis.

References

1. S. Teir, R. Kuusik, C.-J. Fogelholm and R. Zevenhoven, Production of magnesium carbonates from serpentinite for long-term storage of CO_2. *Int. J. Miner. Process.* 85 (2007) 1-15.
2. W. J. J. Huijgen, R. N. J. Comans and G.-J. Witkamp, Cost evaluation of CO_2 sequestration by aqueous mineral carbonation. *Energy Convers. Manage.* 48 (2007) 1923-1935.
3. P. Cho, T. Mattisson and A. Lyngfelt, Comparison of iron-, nickel-, copper- and manganese-based oxygen carriers for chemical-looping combustion. *Fuel* 83 (2004) 1215-1225.
4. A. Lyngfelt, B. Leckner and T. Mattisson, A fluidized-bed combustion process with inherent CO_2 separation; application of chemical-looping combustion. *Chem. Eng. Sci.* 56 (2001) 3101-3113.
5. A. Abad, T. Mattisson, A. Lyngfelt and M. Johansson, The use of iron oxide as oxygen carrier in a chemical-looping reactor. *Fuel* 86 (2007) 1021-1035.
6. C. Linderholm, A. Abad, T. Mattisson and A. Lyngfelt, 160 h of chemical-looping combustion in a 10 kW reactor system with a NiO-based oxygen carrier. *International Journal of Greenhouse Gas Control* 2 (2008) 520-530.
7. P. Cho, T. Mattisson and A. Lyngfelt, Defluidization conditions for a fluidized bed of iron oxide-, nickel oxide-, and manganese oxide-containing oxygen carriers for chemical-looping combustion. *Ind. Eng. Chem. Res.* 45 (2006) 968-977.